

SAINT-ACC: Safety-Aware Intelligent Adaptive Cruise Control for Autonomous Vehicles Using Deep Reinforcement Learning

Lokesh Das¹ Myounggyu Won¹

Abstract

We present an autonomous adaptive cruise control (ACC) system namely SAINT-ACC: Safety-Aware Intelligent ACC system (SAINT-ACC) that is designed to achieve simultaneous optimization of traffic efficiency, driving safety, and driving comfort through dynamic adaptation of the inter-vehicle gap based on deep reinforcement learning (RL). A novel dual RL agent-based approach is developed to seek and adapt the optimal balance between traffic efficiency and driving safety/comfort by effectively controlling the driving safety model parameters and inter-vehicle gap based on macroscopic and microscopic traffic information collected from dynamically changing and complex traffic environments. Results obtained through over 12,000 simulation runs with varying traffic scenarios and penetration rates demonstrate that SAINT-ACC significantly enhances traffic flow, driving safety and comfort compared with the state-of-the-art approach.

1. Introduction

An adaptive cruise control (ACC) enables vehicles to automatically maintain the desired distance to the preceding vehicle by using various kinds of sensors such as radar, LiDAR, and camera (Vahidi & Eskandarian, 2003). It is one of the critical components of autonomous vehicles (Wang et al., 2020). Recent research demonstrates that it can also be used to enhance traffic flow (Ntousakis et al., 2015; Delis et al., 2016; Nikolos et al., 2015) by adaptively adjusting the inter-vehicle gap in response to dynamically changing traffic conditions (Bekiaris-Liberis & Delis, 2019; Goñi-Ros et al., 2019; Das & Won, 2020).

Latest intelligent ACC systems, however, focus mostly on

enhancing traffic flow, overlooking the impact of adaptive adjustment of inter-vehicle gap on driving safety and comfort (Bekiaris-Liberis & Delis, 2019; Goñi-Ros et al., 2019). As such, developing a real-time ACC system that optimizes not only traffic flow but also driving safety and comfort is an important research problem. Recently, a surrogate safety measure (SSM) (Nadimi et al., 2020) such as the time to collision (TTC) model (Gettman & Head, 2003) is incorporated in the design of intelligent ACC systems to account for driving safety and comfort in making a control decision on the inter-vehicle gap (Zhu et al., 2020; Alizadeh et al., 2019). However, we demonstrate that state-of-the-art safety-aware ACC systems (Zhu et al., 2020; Alizadeh et al., 2019) do not perform driving safety assessment effectively under dynamically changing and complex traffic environments (Zhu et al., 2020) because the implications of dynamic adaptation of the critical parameters of the safety model on balancing traffic efficiency and safety are not fully considered.

In this paper, we develop the Safety-Aware Intelligent ACC system (SAINT-ACC), a real-time ACC system designed to perform assessment of driving safety more effectively by dynamically updating the safety model parameters in response to varying traffic conditions through a novel design of a dual reinforcement learning (RL) agent approach aiming to maximize the traffic efficiency, driving safety, and driving comfort simultaneously. Specifically, a separate RL agent is designed to find and adapt the optimal TTC threshold (Gettman & Head, 2003) for the current traffic conditions. This RL agent, by providing the optimal TTC threshold as feedback, interacts with the main RL agent designed to derive an optimal inter-vehicle gap that maximizes traffic flow, driving safety, and comfort all at the same time. In particular, SAINT-ACC makes the control decision on the inter-vehicle gap leveraging rich traffic information including both macroscopic and microscopic traffic information. Furthermore, SAINT-ACC is applicable to different highway types including highways with on-ramps and off-ramps by separately taking into account the traffic as mainline and non-mainline traffic in training the RL agents.

The dual RL agents are trained under various highway scenarios including highways with on-ramps and off-ramps. A

¹Department of Computer Science, University of Memphis, TN, United States. Correspondence to: Myounggyu Won <mwon@memphis.edu>.

simulation platform based on the combination of a traffic simulator, SUMO (Krajzewicz et al., 2012), and a vehicular network simulator, Veins (Sommer et al., 2019), is used to perform extensive simulations over 12,000 runs with varying penetration rates and merging/exiting traffic density to evaluate the performance. Results demonstrate that SAINT-ACC significantly improves traffic efficiency, driving safety, and driving comfort compared with the state-of-the-art intelligent ACC system (Zhu et al., 2020).

2. Related Work

Methods for assessing the safety of autonomous vehicles can be categorized largely into two groups: rule-based approaches and machine learning-based approaches. The rule-based approaches are based on a safety model represented as a function to gauge the level of driving safety. These methods are easy to implement due to simplicity and are capable of assessing driving safety very quickly, thereby being adequate for fast-moving vehicles that should make a control decision affecting driving safety quickly. Nilsson *et al.* design a utility function to determine whether or not it is safe for an autonomous vehicle to change lanes (Nilsson et al., 2016). The utility function computes a utility value based on the average vehicle speed, density of a lane, and the amount of remaining time until the vehicle reaches the end of the lane; If the utility value of a target lane is greater than that of the current lane, changing lanes is considered safe. Zheng *et al.* develop a safety model based on a threshold for deceleration of a lane-changing vehicle and the immediately following vehicle (Zheng et al., 2019). If deceleration of those vehicles is greater than the threshold, it is considered unsafe to change lanes. Rule-based driving safety models are also useful to evaluate the safety of autonomous vehicles. Numerous works utilize the surrogate safety measures (SSM) to evaluate the safety impacts of autonomous vehicle technologies (Morando et al., 2018; Virdi et al., 2019; Rahman & Abdel-Aty, 2018). However, these model-based approaches do not cope well with dynamically changing traffic conditions (Ye et al., 2020).

To address this challenge, recent works are focused on utilizing machine learning techniques in assessing driving safety (Zhu et al., 2020). Numerous research has demonstrated that machine learning-based approaches outperform rule-based approaches in evaluating driving safety (Ye et al., 2020). Mirchevska *et al.* adopt RL which is integrated with a safety verification model to assure that the vehicle action is guaranteed to be safe at any time (Mirchevska et al., 2018). However, their method is designed to make only a binary decision, *i.e.*, whether taking an action is safe or not. Hoel *et al.* adopt a deep Q-Network to allow vehicles to make a lane-changing deci-

sion safely (Hoel et al., 2018). However, a simple reward function is used which considers only extreme cases, *i.e.*, providing a penalizing reward only when a crash occurs; As a result, it does not measure driving safety effectively. Similar RL-based approaches are proposed, *e.g.*, Lin *et al.* utilize deep RL for driving safety in training a merging vehicle to minimize collisions (Lin et al., 2019); Baheri *et al.* incorporate a rule-based model with a dynamically-learned safety module based on RL (Baheri et al., 2019). However, the reward function of these RL-based solutions takes into account only particular dangerous scenarios in giving penalizing rewards, *e.g.*, when merging vehicles stop suddenly or collide. To address this problem, Ye *et al.* develop a solution based on proximal policy optimization (PPO) using deep RL (Ye et al., 2020). Specifically, the reward function incorporates the ‘near-collision’ penalty instead of relying only on the situations where a collision actually occurs. Zhu *et al.* design a better reward function based on human driving data and various other performance criteria such as safety, efficiency, and driving comfort (Zhu et al., 2020). In particular, to evaluate driving safety, a surrogate safety measure called the time to collision (TTC) is incorporated with the reward function. However, a fixed threshold for TTC is used in their model (*i.e.*, 4 seconds), constraining the performance under dynamic traffic conditions. Similarly, Alizadeh *et al.* develop a deep RL agent based on TTC to enable autonomous vehicles to change lanes safely (Alizadeh et al., 2019). However, it also relies on a fixed TTC threshold (1.8 seconds). In contrast to these state-of-the-art research works, we develop a novel dual RL agent approach where the optimal TTC threshold is determined adaptively depending on dynamically changing traffic conditions, which is provided as feedback to the main RL agent for controlling the inter-vehicle gap more effectively.

3. Motivation

A surrogate safety measure (SSM) is an indicator of driving safety. It is used as a tool to assess dangerous driving situations (Nadimi et al., 2020). There are different kinds of SSMs such as time to collision (TTC), unsafe density (UD), proportion of stopping distance (PSD), comprehensive time-based measure (CTM), *etc.* (Guido et al., 2011). The most widely used one is TTC that represents the amount of time remaining until a collision will occur with the front vehicle if the current vehicle keeps its trajectory and speed (Gettman & Head, 2003). More specifically, in this model, a threshold denoted by TTC^* is defined to determine whether or not a collision will occur; Formally, the TTC of the following vehicle F at time t denoted by $TTC_F(t)$ with respect to the leading vehicle L is defined as follows: $TTC_F(t) = \frac{X_L(t) - X_F(t) - l_L}{v_F(t) - v_L(t)}$, $\forall v_F(t) > v_L(t)$, where X , v , and l denote the position, speed, and body

length of a vehicle, respectively. Also, note that TTC is only valid when the speed of the following vehicle F is greater than that of the leading vehicle L (i.e., $v_F(t) > v_L(t)$). According to the TTC model, a dangerous situation is detected at time t if the measured TTC of a following vehicle is smaller than the threshold TTC^* at time t (i.e., $TTC_F(t) < TTC^*$), which indicates that the effectiveness of the TTC model depends on how the threshold TTC^* is determined.

An interesting observation is that state-of-the-art intelligent ACC systems that utilize TTC for evaluating driving safety rely on a fixed TTC threshold (TTC^*) (Zhu et al., 2020; Alizadeh et al., 2019). In this section, we perform a simulation study to understand the effect of TTC^* on the performance of an intelligent ACC system aiming to motivate the needs for a novel method to adapt TTC^* dynamically in response to the current traffic conditions.

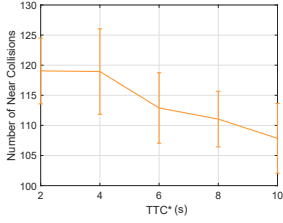


Figure 1. The effect of TTC^* on driving safety.

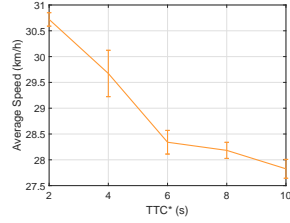


Figure 2. The effect of TTC^* on traffic efficiency.

We implement a state-of-the-art intelligent ACC system using RL integrated with the TTC-based safety model (Zhu et al., 2020). More specifically, in contrast to (Zhu et al., 2020) built upon a fixed TTC^* (i.e., 4 seconds), in this study, we attempt to vary TTC^* to demonstrate the effect of the threshold on the performance of the ACC system in terms of driving safety and traffic efficiency. A highway segment with an on-ramp is created for this simulation study. The details of the simulation settings are described in Section 5. The driving safety is represented as the number of ‘near’ collisions. Here a near collision is defined as a situation where the inter-vehicle gap is smaller than a minimum gap (default 2.5m) (Krajzewicz et al., 2012). Additionally, it is ensured that if the speed of the following vehicle is smaller than or equal to that of the leading vehicle, it is not counted as a near-collision even if the inter-vehicle gap is smaller than the minimum gap. The traffic efficiency is represented by the average vehicle speed.

Fig. 1 shows measured driving safety as a function of TTC^* . We observe that there exists a tradeoff between driving safety and traffic efficiency depending on TTC^* . More specifically, as TTC^* decreases, driving safety degrades. The reason is that some dangerous situations are not de-

tected because TTC^* is small - recall that a dangerous situation is detected when TTC is smaller than TTC^* . In contrast, as shown in Fig. 2, traffic efficiency increases as TTC^* becomes smaller. Another interesting observation is that when TTC^* is too small, the performance gain in terms of driving safety becomes marginal. These results indicate that there exists a TTC^* that strikes the optimal balance between driving safety and traffic efficiency. We can also observe that traffic efficiency can still be improved while sustaining a similar level of driving safety. Therefore, in this paper, we design a novel intelligent ACC system that adapts TTC^* dynamically and uses it to control the inter-vehicle gap to achieve the optimal balance between traffic efficiency and driving safety.

4. SAINT-ACC

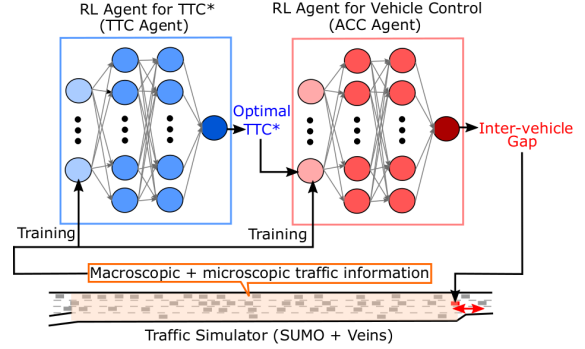


Figure 3. An overview of SAINT-ACC.

An overview of SAINT-ACC is shown in Fig. 3. As shown, SAINT-ACC is built upon a feedback loop between dual RL agents that adapt TTC^* in response to dynamically changing traffic conditions and in turn utilizes the obtained optimal TTC^* to control the inter-vehicle gap to maximize performance. More precisely, SAINT-ACC consists of a RL agent (TTC agent) designed to obtain the optimal TTC^* and another RL agent (ACC agent) to control the inter-vehicle gap. Both agents are trained based on the macroscopic traffic information such as the vehicle density and average vehicle speed as well as microscopic traffic information such as the vehicle length and vehicle acceleration collected from the traffic environment. The TTC agent interacts with the ACC agent continually by providing the optimal TTC^* so that the ACC agent can control the inter-vehicle gap with the most accurate and up-to-date assessment of driving safety to enhance traffic efficiency and driving safety simultaneously.

4.1. Designing the TTC Agent

This section explains the RL framework for training the TTC agent.

State Space: The state space represents the current traffic conditions. It incorporates both the macroscopic and microscopic traffic information including most of the available traffic parameters in the literature, *i.e.*, vehicle acceleration/deceleration, time headway, driving imperfection (according to SUMO (Krajewicz et al., 2012)), minimum inter-vehicle gap, vehicle length, mainline vehicle density, mainline average vehicle speed, non-mainline (*i.e.*, ramp) vehicle density, non-mainline average vehicle speed, and the length of ramp (if applicable). A salient aspect is that the state space distinguishes the traffic parameters for the mainline and non-mainline to generalize application of SAINT-ACC for different highway types, *e.g.*, the non-mainline traffic parameters can be used to represent traffic for various types of ramps.

Action Space: Since the goal of the TTC agent is to find the optimal TTC^* and adapt it dynamically depending on real-time traffic conditions, the action space is primarily designed to control TTC^* . A total of 21 actions are defined with respect to a wide range of values for TTC^* between 0 and 10 with an interval of 0.5. We note that TTC^* greater than 10 is not useful as 10 seconds is enough time to avoid a collision in most highway scenarios (Vogel, 2003).

Reward Function: The reward function denoted by R_{TTC} is the core of the TTC agent which is used to evaluate the efficacy of selected TTC^* . This function is defined based on ‘near’ collisions (as explained in Section 3) and actual collisions in simulation. Specifically, the number of false positives (FP), number of false negatives (FN), and number of actual collisions (AC) are used to determine the reward. A false positive is recorded when the TTC model with the given TTC^* indicates a dangerous situation (*i.e.*, $TTC < TTC^*$) while a near-collision is not registered in simulation. On the other hand, a false negative is recorded when the TTC model with the given TTC^* does not detect a dangerous situation (*i.e.*, $TTC \geq TTC^*$) but a near-collision is registered. Additionally, an actual collision is recorded, if two cars actually crash in simulation. Now the reward function R_{TTC} is calculated as follows: $R_{TTC} = -\alpha_1(\text{Total Number of FPs}) - \alpha_2(\text{Total Number of FNs}) - \alpha_3(\text{Total Number of ACs})$. We set $\alpha_1 = 1$, $\alpha_2 = 2$, and $\alpha_3 = 10$ through numerous simulations to place the high-priority on the number of actual collisions (α_3).

Neural Network: The neural network used to train the TTC agent consists of one hidden layer with 30 neurons.

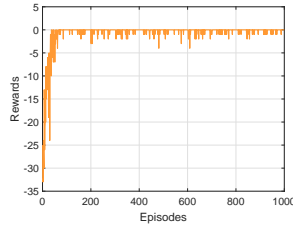


Figure 4. Convergence of the rewards for the TTC agent.

The parameters for the neural network are carefully selected based on the extensive trial and error process which are summarized in Table 1. Especially, we adopt the ϵ -greedy policy (Wunder et al., 2010) to balance between exploration and exploitation in training our neural network. An action is randomly chosen from the action space with probability ϵ , while an action is selected using the greedy method with probability $1 - \epsilon$. It is ensured that ϵ is decreased gradually as the greedy algorithm iterates, *i.e.*, $\epsilon = \max(\epsilon_0 \cdot \lambda_{decay}, \epsilon_{min})$. The parameters ϵ_0 , λ_{decay} , ϵ_{min} chosen for training our neural network are also summarized in Table 1. Fig. 4 displays the rewards for the TTC agent over a large number of episodes, demonstrating the convergence of rewards.

Table 1. Parameters used for the neural network of the TTC Agent.

Neural network architecture	Input size 13 (state size), output size 21 (action size), 1 hidden layer with 30 neurons in each layer, “random_normal” for kernel initialization
Activation functions	ReLU for hidden layer, “linear” for output layer
Replay buffer size	100k samples
$(\gamma, \epsilon_0, \epsilon_{min}, \lambda_{decay})$	(0.95, 1.0, 0.01, 0.99985)
Batch size	64
Loss function	Mean square error (MSE)
Optimization method	Adam with learning rate 0.0001
Target network update frequency	5 episodes (each episode runs for 7 minute of simulation time)
Input Normalization	Batch normalization

4.2. Designing the ACC Agent

The ACC agent is trained to find the optimal inter-vehicle gap to maximize traffic flow, driving safety, and driving comfort. The optimal TTC^* provided by the TTC agent is used as part of the reward function of the ACC agent in making this control decision.

State Space: The state space of the ACC agent is the same as that of the TTC agent since both agents make decision based on traffic information collected from a traffic environment. Specifically, the control decision on the inter-vehicle gap is made based on both the macroscopic and microscopic traffic information.

Action Space: The main goal of the action space is to control the inter-vehicle gap. An action is defined as setting the inter-vehicle gap to a certain value selected from a set of available inter-vehicle gaps. A total of 25 actions corresponding to the headway gaps between 1m and 25m with

an interval of 1m are used. A vehicle takes an action of adjusting the inter-vehicle gap every second in accordance with the current traffic conditions. This dynamic adaptation of the inter-vehicle gap is particularly useful for highways with merging/exiting traffic because creating an appropriate inter-vehicle gap is crucial for merging and exiting vehicles to change lanes smoothly without causing a traffic breakdown that can lead to formation and propagation of a traffic jam. In fact, such a positive effect of adjusting the inter-vehicle gap for preventing a traffic jam has been well studied in the literature (Goñi-Ros et al., 2019).

Reward Function: The reward function of the ACC agent denoted by R_{ACC} consists of three subfunctions defined for driving safety R_s , traffic efficiency R_e , and driving comfort R_c , respectively. In designing the subfunction for driving safety, we employ the approach adopted by the state-of-the-art intelligent ACC system (Zhu et al., 2020) which measures driving safety based on the TTC model as follows: $F_{TTC} = \begin{cases} \log(\frac{TTC}{4}) & \text{if } 0 \leq TTC \leq 4 \\ 0 & \text{otherwise} \end{cases}$, i.e.,

the reward value F_{TTC} is computed based on the TTC value. An interesting aspect is that the TTC threshold TTC^* is fixed to 4 in this model. In contrast, we make two critical modifications: (1) we incorporate the optimal TTC^* which is dynamically adjusted by the TTC agent instead of relying on a fixed value to perform assessment of driving safety more effectively, and (2) we not only consider the driving safety for the ego vehicle but also take into account the driving safety for surrounding vehicles in the given highway segment as a whole. Consequently, our subfunction for driving safety is calculated as follows: $R_s = \begin{cases} \sum_{i \in V} \log(\frac{TTC_i}{TTC^*}) & \text{if } 0 \leq TTC \leq TTC^* \\ 0 & \text{otherwise} \end{cases}$,

where TTC_i indicates the TTC of an individual vehicle i , and V is a set of vehicles in the given highway segment.

The subfunction for traffic efficiency (R_e) is calculated based on the degree of traffic flow which is measured using the average delay to pass a given highway segment. More precisely, if the average delay is greater than the expected delay under congested traffic conditions (which is known priori), a penalizing reward is imposed. On the other hand, if the average delay is smaller than that for congested traffic conditions, a positive reward is given. Consequently, the subfunction for traffic efficiency is defined as follows:

$$R_e = \begin{cases} +1 & \text{if avg delay} \leq \frac{\text{highway length}}{\text{avg speed under congestion}} \\ -1 & \text{if avg delay} > \frac{\text{highway length}}{\text{avg speed under congestion}} \end{cases}.$$

Lastly, the subfunction for driving comfort (R_c) is defined based on an existing driving comfort model (Zhu et al., 2020; Jacobson et al., 1980). In this driving comfort model, the level of driving comfort is quantified using the change

rate of acceleration called Jerk as follows: $R_c = -\frac{\text{jerk}^2}{27.04}$. Here, since our sampling interval is one second (i.e., vehicles make a control decision on the inter-vehicle gap every second), and the acceleration is bounded between -2.6 and 2.6 m/s², the greatest possible jerk is $\frac{2.6 - (-2.6)}{1.0} = 5.2$. As such, to bound the result of R_c between 0 and 1, we divide by 27.04 which is the square of the greatest possible jerk.

Now combining all three subfunctions, the reward function R_{ACC} is defined as follows: $R_{ACC} = \beta_1 R_e + \beta_2 R_s + \beta_3 R_c$, where, β_1, β_2 , and β_3 are weighting parameters which can be used to allow the user to vary the weight on a certain performance criteria. In our simulation, we use $\beta_1 = \beta_2 = \beta_3 = 1$ to optimize traffic efficiency, driving safety, and driving comfort with the same weight.

Neural Network: The neural network of the ACC agent is similar to that of the TTC agent. Through trial and error, however, we find that the following configuration is more effective for the ACC agent: we use one hidden layer with 30 neurons; the replay buffer size is 100k samples; and the batch size is 64. We also adopt the ϵ -greedy policy (Wunder et al., 2010) for training the neural network for the ACC agent with a slightly smaller λ_{delay} . Fig. 5 shows the reward values as a function of episodes demonstrating the convergence of rewards for the ACC agent.

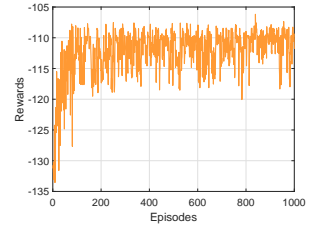


Figure 5. Convergence of the rewards for the ACC agent.

5. Results

We implement SAINT-ACC and the state-of-the-art approach (referred to as ‘Zhu’ hereafter) (Zhu et al., 2020) on a traffic simulation framework, SUMO (Krajzewicz et al., 2012), which is integrated with a vehicular network simulator, Veins (Sommer et al., 2019). The RL framework for SAINT-ACC and Zhu (Zhu et al., 2020) are implemented using Python based on Keras and Tensorflow (Abadi et al., 2016); It is interfaced with SUMO via Traffic Control Interface (TraCI) (Wegener et al., 2008). Simulations are performed with a PC running MacOS (Majove 10.14.5) with a 1.4GHz Intel Core i5 CPU and 8GB of RAM.

We consider two most common highway types, i.e., a highway segment with an on-ramps and that with an off-ramp. We create a 1.5km highway segment with a ramp with the length of 360m. There is also a 180m-long acceleration lane that is used by vehicles to accelerate to merge into the mainline. Traffic is generated and injected to the main road at a rate of 1800 veh/h/lane. A vehicle used for this

simulation has the body length of 4~5m and changes lanes based on a widely adopted lane-changing model (Erdmann, 2015). SAINT-ACC allows vehicles to take an action of controlling the inter-vehicle gap every one second in response to dynamically changing traffic conditions. In particular, the minimum headway distance for each vehicle is intentionally set to 0m to permit collisions in simulation for the purpose of evaluating driving safety. Also, both the maximum acceleration and deceleration of a vehicle are set to sufficiently high to evaluate driving comfort effectively considering the fact that the maximum acceleration and deceleration to ensure driving comfort is within the range between 2 m/s^2 and 3 m/s^2 (Hoberock, 1976). The performance of SAINT-ACC is compared with Zhu and the baseline method (referred to as 'Base' hereafter). In the baseline method, vehicles are not equipped with any intelligent ACC technology. We measure driving safety, traffic efficiency, and driving comfort by varying the technology penetration rate, vehicle density on the on-ramp as well as off-ramp. Specifically, driving safety is measured based on the number of near-collisions as defined in Section 3; Traffic efficiency is measured using the average speed of vehicles in the highway segment; And driving comfort is measured based on the acceleration and deceleration of vehicles.

5.1. A Highway with an On-ramp

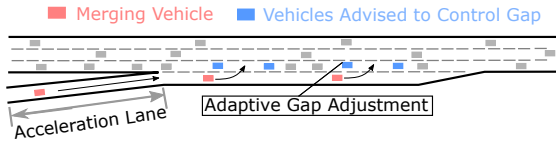


Figure 6. Illustration of a highway segment with on-ramp.

A highway with an on-ramp is considered for performance evaluation. A top view is depicted in Fig. 6 showing that blue-colored vehicles adjust the inter-vehicle gap to allow merging vehicles marked as red color to change lanes more smoothly in such a way that driving safety, traffic efficiency, and driving comfort are improved. In this simulation study, we measure the performance of SAINT-ACC, Zhu, and Base by varying the penetration rate. For each penetration rate, we run 200 random simulations to represent a single data point.

Fig. 7 shows the results on driving safety. No significant patterns are observed regarding driving safety for Base because no vehicle is equipped with an intelligent ACC system. On the other hand, both SAINT-ACC and Zhu achieve significantly better driving safety compared with Base. Specifically, SAINT-ACC achieves by up to 99.2% higher driving safety than that of Base when the penetration rate is 80%. It is also observed that SAINT-ACC also performs significantly better than Zhu by up to 42.4%.

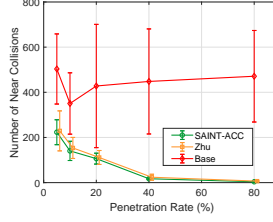


Figure 7. Driving safety for highway with on-ramp.

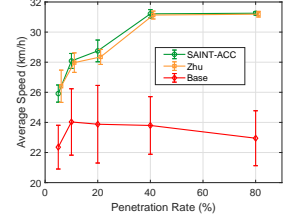


Figure 8. Traffic efficiency for highway with on-ramp.

These results demonstrate the efficacy of adaptively adjusting TTC^* and using it to control the inter-vehicle gap, while Zhu relies on a fixed TTC^* . However, interestingly, the performance gap between SAINT-ACC and Zhu becomes smaller as the penetration rate increases. The reason is because, with a higher penetration rate, there are fewer vehicles without an intelligent ACC system, and these vehicles are the cause for degraded driving safety.

Fig. 8 depicts the results on traffic efficiency. Both SAINT-ACC and Zhu have significantly higher traffic efficiency compared with Base because they adapt the inter-vehicle gap so that merging vehicles change the lane to the mainline smoothly with reduced interruption to traffic flow of the mainline. The average speed of SAINT-ACC is higher by up to 36.2% compared with Base when the penetration rate is 80%. It is also observed that SAINT-ACC achieves higher average vehicle speed compared with Zhu in all penetration rates by up to 3.57%. This result demonstrates that there is still a room for improving traffic efficiency while sustaining superior driving safety by adaptively adjusting TTC^* .

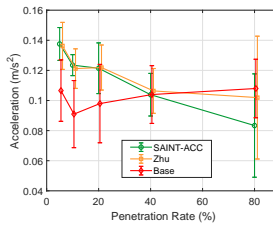


Figure 9. Driving comfort for highway with on-ramp.

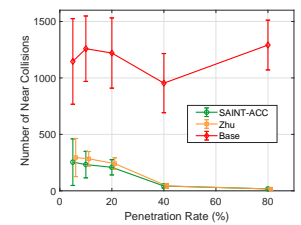


Figure 10. Driving safety for highway with off-ramp.

Fig. 9 shows the results on driving comfort. The literature shows that the maximum acceleration and deceleration to assure comfortable driving is in the range between 2 m/s^2 and 3 m/s^2 (Hoberock, 1976). As such, we observe that driving comfort is not significantly impacted by all approaches regardless of the penetration rate. An interesting observation is that when the penetration rate is small (*i.e.*, smaller than 40%), both SAINT-ACC and Zhu have lower driving comfort level compared with that of Base. The rea-

son is possibly that when vehicles adjust the inter-vehicle gap to allow merging vehicles to change lanes, the following vehicles that are not equipped with an intelligent ACC system need to decrease their speed significantly, causing degradation of driving comfort. We also observe that driving comfort for both SAINT-ACC and Zhu keep improving with higher penetration rates. When most vehicles are equipped with an intelligent ACC system, we observe that both approaches provide much more comfortable driving experience. In particular, SAINT-ACC has 18.2% higher driving comfort level than that of Zhu when the penetration rate is 80%.

5.2. Highway with Off-ramp

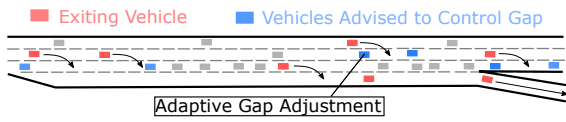


Figure 11. Illustration of a highway segment with off-ramp.

We now evaluate the performance of SAINT-ACC on a highway with an off-ramp (A top view depicted in Fig. 11). In particular, vehicles exiting the highway are randomly selected from all three lanes of the main road. Fig. 10 shows the results on driving safety. Similar to the results for the highway with an on-ramp, no significant pattern of driving safety with varying penetration rate is observed for Base because no vehicle is equipped with an intelligent ACC system. In contrast, as the penetration rate increases, driving safety is enhanced for both SAINT-ACC and Zhu. The driving safety for SAINT-ACC is significantly higher compared with Base by up to 98.7% which indicates that dynamic adjustment of the inter-vehicle gap allows exiting vehicles to change lanes smoothly to exit the highway. In particular, in comparison with Zhu, we note that SAINT-ACC has improved driving safety especially with smaller penetration rates, *i.e.*, by up to 13.8% when the penetration rate is 5%. On the other hand, as the penetration rate becomes higher, the performance gap between SAINT-ACC and Zhu becomes smaller, which can be explained with the similar reason for the on-ramp scenario.

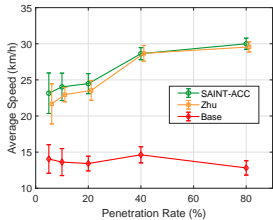


Figure 12. Traffic efficiency for highway with off-ramp.

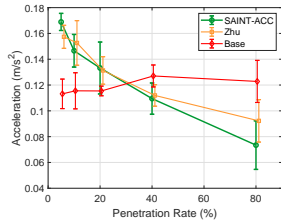


Figure 13. Driving comfort for highway with off-ramp.

Fig. 12 shows the results on traffic efficiency. Both SAINT-ACC and Zhu have significantly higher traffic efficiency than Base, especially as the penetration rate increases. In particular, SAINT-ACC has higher traffic efficiency by up to 134.2% compared with Base. This result demonstrates that SAINT-ACC enables exiting vehicles to change lanes to exit the highway without causing much interruption to surrounding vehicles since the inter-vehicle gap is appropriately adjusted. We also observe that as the penetration rate increases, the traffic efficiency of both SAINT-ACC and Zhu increases. Especially, the performance gap between the two approaches becomes greater when the penetration is small; It is observed that SAINT-ACC achieves higher traffic efficiency by up to 6.82% compared with Zhu.

Fig. 13 shows the results on driving comfort. Similar results as those for the highway with an on-ramp are observed. Specifically, the impact of exiting vehicles on driving comfort is insignificant. Despite such a small impact, driving comfort for both SAINT-ACC and Zhu keeps increasing as the penetration rate increases. Compared with Base, SAINT-ACC improves the driving comfort level by up to 40.2% when the penetration is as high as 80%. However, when the penetration rate is small (*e.g.*, < 30%), the driving comfort for SAINT-ACC becomes even worse than that for Base. The reason is because the following vehicles without an intelligent ACC system have to accelerate/decelerate as the front vehicle equipped with SAINT-ACC or Zhu adjusts the inter-vehicle gap.

5.3. Effect of Merging Traffic

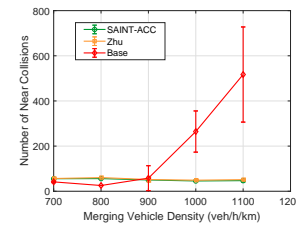


Figure 14. Effect of merging traffic on driving safety.

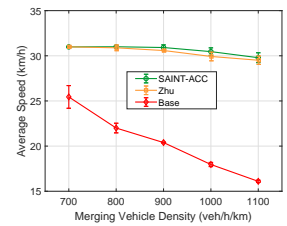


Figure 15. Effect of merging traffic on traffic efficiency.

Merging traffic is one of the main causes for traffic congestion (Milanés et al., 2010). We evaluate the performance of SAINT-ACC by varying the merging traffic density. Fig. 14 displays the driving safety of all three approaches as a function of the merging vehicle density. The results show that the driving safety of Base degrades when there are more merging vehicles. The traffic also becomes very unstable as the merging vehicle density increases as indicated by the large standard deviation. In contrast, both SAINT-ACC and Zhu successfully suppress the number of near-collisions even if the merging vehicle density is very high. Specifically, SAINT-ACC improves driving safety by up to 93.6%

compared with Base, indicating that SAINT-ACC manages effectively complex traffic conditions with very high merging vehicle density. In comparison with Zhu, SAINT-ACC achieves higher driving safety by up to 8.7% which demonstrates the effectiveness of dynamically adjusting TTC^* .

Fig. 15 shows the results on traffic efficiency. It is observed that when no intelligent ACC solution is applied, traffic efficiency degrades as the merging vehicle density increases. In contrast, both SAINT-ACC and Zhu successfully sustain high average vehicle speed. In particular, SAINT-ACC achieves higher average speed by up to 83.9% compared with that of Base, demonstrating the effectiveness of dynamic adaptation of the inter-vehicle gap in response to varying merging vehicle density. We also observe that SAINT-ACC achieves higher traffic efficiency compared with Zhu.

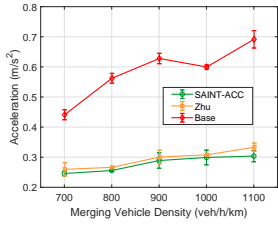


Figure 16. Effect of merging traffic on driving comfort.

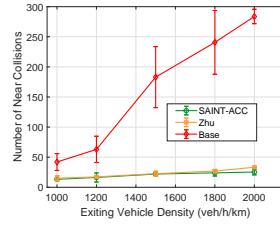


Figure 17. Effect of exiting traffic on driving safety.

We observe that the driving comfort level decreases for all three approaches as the merging vehicle density increases (Fig. 16). It is also observed that both SAINT-ACC and Zhu improve the driving comfort level compared with Base. However, we note again that the results are insignificant as the average acceleration of the vehicles is sufficiently in the range of the acceleration for comfortable driving (Hoerock, 1976) regardless of the merging vehicle density.

5.4. Effect of Exiting Traffic

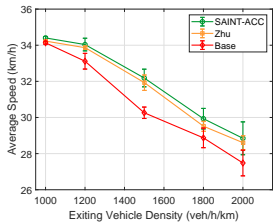


Figure 18. Effect of exiting traffic on traffic efficiency.

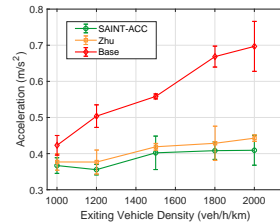


Figure 19. Effect of exiting traffic on driving comfort.

Exiting traffic is another important cause for traffic congestion (Günther et al., 2012). We evaluate the performance of SAINT-ACC by varying the exiting traffic density. In

particular, exiting vehicles are randomly selected from all three lanes of the main road. Fig. 17 shows the effect of exiting traffic density on driving safety. It can be seen that driving safety of Base significantly degrades as there are more vehicles exiting the highway. In contrast, both SAINT-ACC and Zhu keep the number of near-collisions fairly small although the exiting vehicle density increases. Especially, SAINT-ACC enhances driving safety by up to 91.5% compared with Base. Furthermore, SAINT-ACC has better driving safety in comparison with Zhu as well, specifically by up to 24% when the exiting vehicle density is 2,000 veh/h. These results demonstrate the advantages of adjusting the inter-vehicle gap dynamically using the optimal TTC^* in response to dynamic traffic conditions.

Fig. 18 depicts the results on traffic efficiency. We observe that the traffic efficiency of all three approaches decreases as the exiting vehicle density increases. We also observe that traffic efficiency is less significantly influenced by exiting traffic compared to merging traffic. Although we have more exiting vehicles, they are randomly distributed on all three lanes in contrast to merging vehicles that are all on the merging lane significantly affecting the traffic flow on the lane adjacent to the on-ramp. Overall, compared with Base and Zhu, SAINT-ACC improves the traffic flow by up to 11.8% and 4.1%, respectively. Fig. 19 displays the results on driving comfort which demonstrate that SAINT-ACC improves the driving comfort level by up to 41.3% and 7.6% in comparison with Base and Zhu, respectively.

5.5. Computational Delay

To demonstrate that SAINT-ACC is capable of making a control decision well within the one-second update interval, we measure the computational delay needed to make a control decision. The delay is

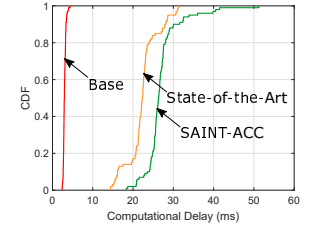


Figure 20. Computation delay.

measured 100 times per each epoch for SAINT-ACC, Zhu, and Base. Fig. 20 depicts the cumulative distribution function (CDF) graph of the computational delay. The average computational delays for Base, Zhu, and SAINT-ACC are 3ms, 22.3ms, 26.9ms, respectively. It is observed that Base computes the inter-vehicle distance very quickly since it is simply a standard ACC system. On the other hand, SAINT-ACC and Zhu take more time to make a control decision on the inter-vehicle gap as they run the RL framework. Especially, in comparison with Zhu, the computational delay for SAINT-ACC is 17% higher on average. However, the average computation time for SAINT-ACC is still sufficiently small for vehicles to make a decision every one-second update interval.

6. Conclusion

We have presented SAINT-ACC, a safety-aware intelligent ACC system designed to maximize traffic efficiency, driving safety, and driving comfort simultaneously by obtaining and adjusting the optimal TTC threshold that is in turn used to control the inter-vehicle gap adaptively in response to dynamically changing traffic conditions. To the best of our knowledge, this is the first intelligent ACC system that strikes the optimal balance between traffic efficiency and driving safety/comfort. Our future work is to implement a proof-of-concept SAINT-ACC system on a real vehicle platform and perform experiments to validate the performance of SAINT-ACC under real-world traffic environments using open-source semi-autonomous driving systems such as Comma.AI (Santana & Hotz, 2016).

References

- Abadi, M., Agarwal, A., Barham, P., Brevdo, E., Chen, Z., Citro, C., Corrado, G. S., Davis, A., Dean, J., Devin, M., et al. Tensorflow: Large-scale machine learning on heterogeneous distributed systems. *arXiv preprint arXiv:1603.04467*, 2016.
- Alizadeh, A., Moghadam, M., Bicer, Y., Ure, N. K., Yavas, U., and Kurtulus, C. Automated lane change decision making using deep reinforcement learning in dynamic and uncertain highway environment. In *Intelligent Transportation Systems Conference (ITSC)*, pp. 1399–1404, 2019.
- Baheri, A., Nagesh Rao, S., Tseng, H. E., Kolmanovsky, I., Girard, A., and Filev, D. Deep reinforcement learning with enhanced safety for autonomous highway driving. *arXiv preprint arXiv:1910.12905*, 2019.
- Bekiaris-Liberis, N. and Delis, A. Feedback control of freeway traffic flow via time-gap manipulation of ACC-equipped vehicles: A PDE-based approach. *IFAC-PapersOnLine*, 52(6):1–6, 2019.
- Das, L. and Won, M. D-ACC: dynamic adaptive cruise control for highways with on-ramps based on deep q-learning. *arXiv preprint arXiv:2006.01411*, 2020.
- Delis, A. I., Nikolos, I. K., and Papageorgiou, M. Simulation of the penetration rate effects of acc and cacc on macroscopic traffic dynamics. In *International Conference on Intelligent Transportation Systems (ITSC)*, pp. 336–341, 2016.
- Erdmann, J. Sumo’s lane-changing model. In *Modeling Mobility with Open Data*, pp. 105–123. 2015.
- Gettman, D. and Head, L. Surrogate safety measures from traffic simulation models. *Transportation Research Record*, 1840(1):104–115, 2003.
- Goñi-Ros, B., Schakel, W. J., Papacharalampous, A. E., Wang, M., Knoop, V. L., Sakata, I., van Arem, B., and Hoogendoorn, S. P. Using advanced adaptive cruise control systems to reduce congestion at sags: An evaluation based on microscopic traffic simulation. *Transportation Research Part C: Emerging Technologies*, 102:411–426, 2019.
- Guido, G., Saccomanno, F., Vitale, A., Astarita, V., and Festa, D. Comparing safety performance measures obtained from video capture data. *Journal of Transportation Engineering*, 137(7):481–491, 2011.
- Günther, G., Coeymans, J. E., Muñoz, J. C., and Herrera, J. C. Mitigating freeway off-ramp congestion: A surface streets coordinated approach. *Transportation Research Part C: Emerging Technologies*, 20(1):112–125, 2012.
- Hoberock, L. L. A survey of longitudinal acceleration comfort studies in ground transportation vehicles. Technical report, Council for Advanced Transportation Studies, 1976.
- Hoel, C.-J., Wolff, K., and Laine, L. Automated speed and lane change decision making using deep reinforcement learning. In *International Conference on Intelligent Transportation Systems (ITSC)*, pp. 2148–2155, 2018.
- Jacobson, I. D., Richards, L. G., and Kuhlthau, A. R. Models of human comfort in vehicle environments. *Human Factors in Transport Research*, 2, 1980.
- Krajzewicz, D., Erdmann, J., Behrisch, M., and Bieker, L. Recent development and applications of SUMO-Simulation of Urban MObility. *International Journal on Advances in Systems and Measurements*, 5(3&4), 2012.
- Lin, Y., McPhee, J., and Azad, N. L. Anti-jerk on-ramp merging using deep reinforcement learning. *arXiv preprint arXiv:1909.12967*, 2019.
- Milanés, V., Godoy, J., Villagrà, J., and Pérez, J. Automated on-ramp merging system for congested traffic situations. *IEEE Transactions on Intelligent Transportation Systems*, 12(2):500–508, 2010.
- Mirchevska, B., Pek, C., Werling, M., Althoff, M., and Boedecker, J. High-level decision making for safe and reasonable autonomous lane changing using reinforcement learning. In *International Conference on Intelligent Transportation Systems (ITSC)*, pp. 2156–2162, 2018.
- Morando, M. M., Tian, Q., Truong, L. T., and Vu, H. L. Studying the safety impact of autonomous vehicles using simulation-based surrogate safety measures. *Journal of Advanced Transportation*, 2018, 2018.

-
- Nadimi, N., NaserAlavi, S. S., and Asadamraji, M. Calculating dynamic thresholds for critical time to collision as a safety measure. In *Proceedings of the Institution of Civil Engineers-Transport*, pp. 1–21, 2020.
- Nikolos, I. K., Delis, A. I., and Papageorgiou, M. Macroscopic modelling and simulation of ACC and CACC traffic. In *International Conference on Intelligent Transportation Systems (ITSC)*, pp. 2129–2134, 2015.
- Nilsson, J., Silvlin, J., Brannstrom, M., Coelingh, E., and Fredriksson, J. If, when, and how to perform lane change maneuvers on highways. *IEEE Intelligent Transportation Systems Magazine*, 8(4):68–78, 2016.
- Ntousakis, I. A., Nikolos, I. K., and Papageorgiou, M. On microscopic modelling of adaptive cruise control systems. *Transportation Research Procedia*, 6:111–127, 2015.
- Rahman, M. S. and Abdel-Aty, M. Longitudinal safety evaluation of connected vehicles’ platooning on expressways. *Accident Analysis & Prevention*, 117:381–391, 2018.
- Santana, E. and Hotz, G. Learning a driving simulator. *arXiv preprint arXiv:1608.01230*, 2016.
- Sommer, C., Eckhoff, D., Brummer, A., Buse, D. S., Hagenauer, F., Joerer, S., and Segata, M. Veins: The open source vehicular network simulation framework. In *Recent Advances in Network Simulation*, pp. 215–252. Springer, 2019.
- Vahidi, A. and Eskandarian, A. Research advances in intelligent collision avoidance and adaptive cruise control. *IEEE Transactions on Intelligent Transportation Systems*, 4(3):143–153, 2003.
- Virdi, N., Grzybowska, H., Waller, S. T., and Dixit, V. A safety assessment of mixed fleets with connected and autonomous vehicles using the surrogate safety assessment module. *Accident Analysis & Prevention*, 131:95–111, 2019.
- Vogel, K. A comparison of headway and time to collision as safety indicators. *Accident Analysis & Prevention*, 35(3):427–433, 2003.
- Wang, C., Gong, S., Zhou, A., Li, T., and Peeta, S. Cooperative adaptive cruise control for connected autonomous vehicles by factoring communication-related constraints. *Transportation Research Part C: Emerging Technologies*, 113:124–145, 2020.
- Wegener, A., Piórkowski, M., Raya, M., Hellbrück, H., Fischer, S., and Hubaux, J.-P. TraCI: an interface for coupling road traffic and network simulators. In *Communications and Networking Simulation Symposium*, pp. 155–163, 2008.
- Wunder, M., Littman, M. L., and Babes, M. Classes of multiagent Q-learning dynamics with epsilon-greedy exploration. In *International Conference on Machine Learning (ICML-10)*, pp. 1167–1174, 2010.
- Ye, F., Cheng, X., Wang, P., and Chan, C.-Y. Automated lane change strategy using proximal policy optimization-based deep reinforcement learning. *arXiv preprint arXiv:2002.02667*, 2020.
- Zheng, Y., Ran, B., Qu, X., Zhang, J., and Lin, Y. Cooperative lane changing strategies to improve traffic operation and safety nearby freeway off-ramps in a connected and automated vehicles environment. *IEEE Transactions on Intelligent Transportation Systems*, 2019.
- Zhu, M., Wang, Y., Pu, Z., Hu, J., Wang, X., and Ke, R. Safe, efficient, and comfortable velocity control based on reinforcement learning for autonomous driving. *Transportation Research Part C: Emerging Technologies*, 117:102662, 2020.